LAWRENCE
LIVERMORE
NATIONAL
LABORATORY

LLNL-CONF-656341

Ultrafast Dynamic Response of Single Crystal PETN and Beta-HMX

J. M. Zaug, M. R. Armstrong, J. C. Crowhurst, L. Feranti, R. Swan, R. Gross, N. E. Teshlich, M. Wall, R. A. Austin, L. E. Fried

July 1, 2014

International Detonation Symposium #15
San Francisco, CA, United States
July 13, 2014 through July 18, 2014

Disclaimer

Ultrafast Dynamic Response of Single Crystal PETN and Beta-HMX

Joseph M. Zaug[*], Michael R. Armstrong[*], Jonathan C. Crowhurst[*], Louis Ferranti[*], Raymond Swan[*], Richard Gross[*], Nick E. Teslich Jr.[*], Mark A. Wall[*], Ryan A. Austin[*] and Laurence E Fried[*]

[*]Lawrence Livermore National Laboratory, Livermore, CA, 94551

Abstract. We report 100 ps time-scale compression wave speeds from shock impacted single crystal PETN and beta-HMX. The ultrafast compression rise-time and the high temporal fidelity of our time-domain interferometry measurements enable characterization of the anisotropic dynamic response of energetic materials. Wave speed is measured during the first few microns of lateral propagation into a crystal and prior to the onset of shock induced initiation. Single crystal wave speeds reveal a clear anisotropic dynamic response. For propagation in the direction normal to the (110) crystallographic plane we measure predominately elastic component wave speeds. Below 12 GPa, wave propagation speeds in the direction normal to the (010) plane in beta-HMX overlap with established shock Hugoniot and static measurements. The (010) ultrafast data also match well with scaled PBX9501 data that extend up to 15 GPa. For shock pressures that exceed 12 GPa along the HMX crystallographic b-axis, wave speeds increase along an established line while gas gun and diamond-anvil cell derived values increase sublinearly. At 26 GPa the slope, $dU_S\, dU_P^{-1}$ decreases for ultrafast shock data: the commensurate drop in volume may be attributed to a previously reported phase transition. These results guide the development of crystal plasticity models.

Introduction

A general premise of energetic materials (EMs) continuum scale modeling efforts is that understanding the nature of shocked solid-phase formulations on the 1 – 100 ps timescales and sub-micron to micron length scales will enable more accurate (non-empirical) physciochemical predictions up to time and length scales consistent with chemical equilibrium product states that persist behind a steady detonation wave. The work presented here begins to explore the dynamic response of solid-phase EMs on the 100 ps timescale. Another motivation driving this work is to extend the range of measured EM unreacted shock Hugoniot states. If one can shock solid explosives on an ultrafast timescale and measure wave propagation speeds with a sufficiently high temporal fidelity, then principal (unreacted) Hugoniot states can be probed at higher particle velocities (*Up*) than otherwise possible using longer time scale experimental platforms. When conducting ultrafast timescale studies care must be taken to measure wave speeds and also to properly attribute the type of wave being measured. Tabletop ultrafast shockwave measurements are complementary to gas gun shock studies; and ideally, both platforms are utilized in concert so as to more comprehensively learn how microstructure e.g., lattice defects and voids, affects the dynamic

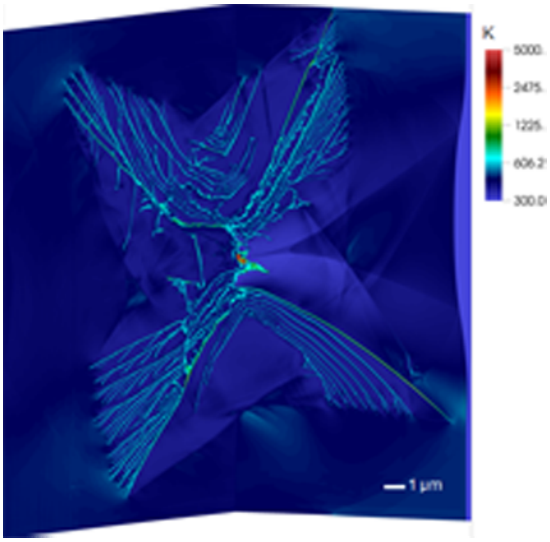

Fig. 1. A simulated temperature field profile of a shock collapsed 1-µm diameter pore embedded in single crystal beta-HMX. The shear bands radiating away from the collapsing pore (center) result from localized deformation. The crystal model restricts plastic deformation (slip) to certain crystallographic planes and also allows for the observed melting within the propagating bands.

response of shocked materials over a seven-fold or more decadal range in strain rate and compression time. Here we report on the dynamic response of PETN and beta-HMX single crystals to ultrafast compression along different crystallographic directions. Single crystal EMs were chosen for this study because of their relatively low defect density and void fraction. Moreover, one can begin to characterize anisotropic wave propagation phenomena on < 10 mg EM samples that are well-suited for study using tabletop laser shock systems. The reported experimental results provide, albeit with higher strain rates than gun experiments, new physical insight and therefore guidance to theoretical efforts aimed at modelling the plastic response of shocked solid-phase EMs and EM formulations (See Fig. 1).

Experimental Details

Sample Preparation

We began by cleaving ~100 mg single crystals to yield approximately 20 mg daughter crystals. PETN samples were cleaved along the (110) crystal plane and beta-HMX crystals were cleaved along (110) and (010) crystal faces. Daughter crystals were polished down to < 10 mg. They were then polished again by hand to a lateral thickness of ~ 1 mm using 3 µm Al_2O_3 paper. This intermediate polishing sequence was completed using 1 µm Al_2O_3 paper. (No fluid carrier was used.). At this point, single crystals were mounted into an annulus using UV cured epoxy. The free surface of the mounted crystal was lapped mechanically using a nylon cloth and a series of diamond lapping suspensions ranging from 9 to 1 µm particle size. The final lapping sequence was conducted on a short-nap cloth using a colloidal silica suspension. Once the final lapping sequence was completed and the crystal surface was dried using house-supplied nitrogen gas, a 50 nm thick layer of polystyrene was spin coated onto the crystal surface. Next a TEM grid (mask) was secured to the polished side of the crystal and then approximately 1 µm of aluminum (containing ~ 5% wt. oxygen) was sputtered onto the surface using a Gatan Precision Etching Coating System. After the aluminum deposition sequence was completed the TEM mask was removed. A grid of 125 x 125 µm Al ablators remains (See Fig. 2). PETN and HMX sample assemblies were stored in a desiccator (~20% humidity).

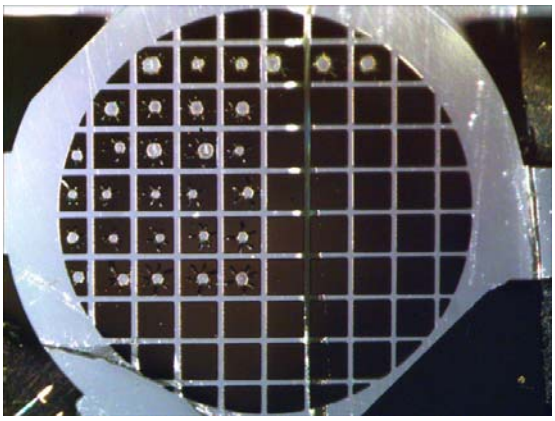
Fig. 2. A completed beta-HMX sample assembly. Here we see that 30 ultrafast shock measurements have been completed on this particular sample.

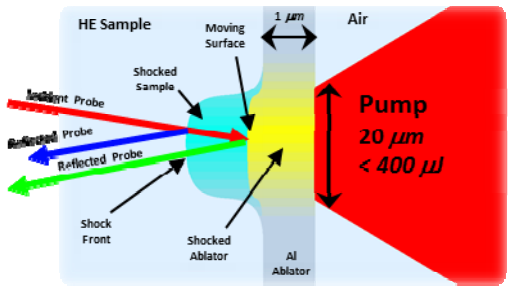

Fig. 3. Schematic diagram of the pump-probe geometry. To enhance clarity the diagram is not drawn to scale.

Ultrafast Shocks and Measurements

The ultrafast shock experimental technique used in this study has been described in great detail[1]. We use a chirped pulse amplification system (CPA) to generate a single laser pump pulse (< 400 μJ pulse energy, ~350 ps pulse-width, ~25 nm bandwidth, ~12 ps width rise time) to launch a shock wave within a ~1 μm thick aluminum ablator. A shock wave propagates through the ablator and breaks out into an energetic material. A small fraction of the CPA pulse energy is diverted and split into a probe pair that are separated in time and focused in a collinear fashion onto a propagating shock wave (See Fig. 3). The probe pulses partially backreflect off of the propagating shock wave and also from the surface of the propagating ablator or piston. In our experiments, the velocity of the shock front exceeds the piston velocity and so an etalon forms with a time varying and increasing path length (width). The rate of change between the optical phase of each backreflected probe pulse results in a sinusoidal beating pattern. The frequency of the sinusoid is proportional to the shock velocity. The selected time separation between each probe pulse (10 ps) determines the intrinsic temporal fidelity (maximum number of fringes that may be recorded during the transit or duration of the optical pulse) of our interferometric data. The passage of time is encoded within the chirped pulses: linearly dispersed wavelength components are transformed discretely into time using an imaging spectrograph. A CCD detector records the time dependent phase and intensity data. CCD pixel columns record time and the CCD pixel rows record spatial information. For this study one row pixel = ~ 2 um and one column pixel = 0.26 ps. A series of non-pump images are recorded and averaged to provide zero-phase (no displacement) calibration data. The intensity of the offset in the phase modulated signal is proportional to the piston velocity. Raw CCD images were read into a MatLab script written to generate and further process time dependent phase results. A moving average window is applied to the time trace data in order to filter-out high frequency noise. The time resolution of our data ultimately depends on the temporal width of the moving window: in this study the time resolution is ~10.3 ps.

Data Reduction

In Figure 4 we present an ultrafast time scale trace from shocked (010) beta-HMX. To process ultrafast time domain interferometric data from an optically transparent material we first select a temporal window where the sinusoidal oscillation frequency and intensity offset are relatively stable. Within the truncated region we fit the data using a sine function (linear background) to determine the oscillation period, (τ) red curve; the oscillation amplitude, ($\Delta\delta_{max}$); and, the phase intensity offset, ($\Delta\theta_m$) green dashed line. From these three

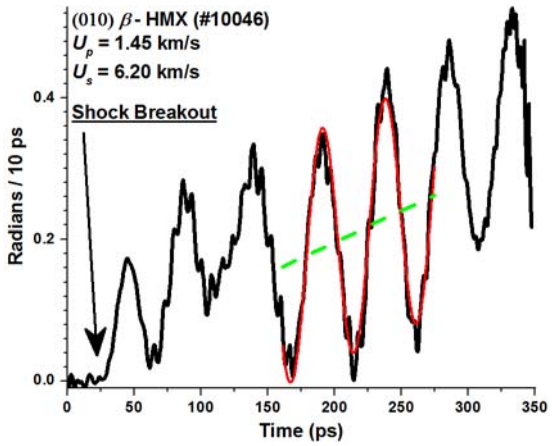

Fig. 4. A randomly selected time domain interferometry trace from beta-HMX shocked in a direction normal to the (010) plane. The laser pump pulse energy was 375 μJ. The shock pressure determined from the fit (red solid curve, green dashed line) is 17.0 GPa.

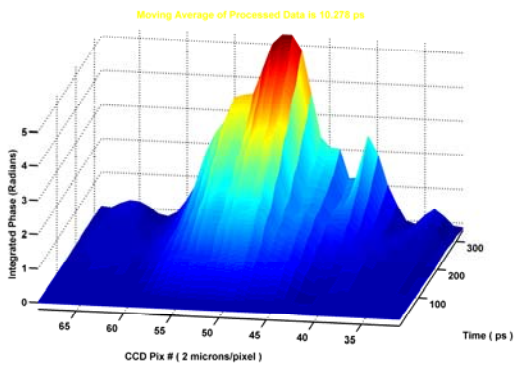

Fig. 5. The time dependent optical phase displacement profile from which shock wave parameters were computed in Fig. 4.. The relative change in phase is measured in 10 ps increments. The time trace in Fig. 4 was computed by integrating data in pixel row # 50.

parameters –assuming a reasonably constant 1D wave front profile– one can determine the shock U_S, and piston U_P, velocity including the index of refraction, n_s, behind a shock front.

For the highest magnitude shock velocities measured in this experiment, wave propagation into the EM is < 2.5 μm. The radius of curvature near the end of the pump pulse duration is nominally 50 μm. Therefore the maximum propagation distance is approximately 5% of the radius of curvature of the shock front. In this study we integrated phase displacement data along the center pixel where maximum shock breakout occurs (See Fig. 5). We further demonstrate that integrating, for example, nine CCD rows with maximum phase displacement from shocked PETN can yield essentially the same results as compared to fourteen separate shots where we integrate along one pixel row of maximum displacement. This approach was previously demonstrated on polycrystalline PETN[2].

The error estimates given for single-shot data points plotted in the U_S-U_P plane are the residual differences between each point and a line fit to all points. For (010) HMX two lines were fit: one for data below 26 GPa and one for data above 26 GPa. Binned data point errors are generated in the same way. The minimum number of points per bin was determined iteratively over a points/bin range of 2-8. The minimum points/bin result with the lowest

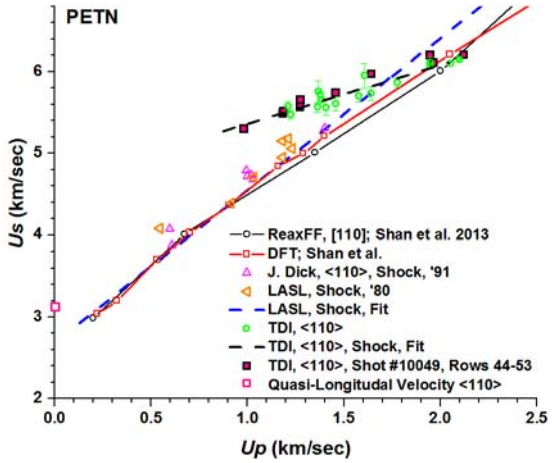

Fig. 6. A comparison of TDI single crystal (110) PETN shock data with previous gas gun data[3] from shocked polycrystalline and single crystal (110) PETN[4] including more recent theoretical results[5].

absolute sum total standard deviation value is selected.

Experimental Results

We conducted ultrafast shock experiments on a (110) PETN crystal. Fourteen separate time domain interferometry (TDI) measurements were conducted (See Fig. 6). Time dependent phase displacement profiles were integrated along the CCD row with the maximum cumulative displacement. One shock profile, (shot # 10049), was integrated along nine different CCD rows. Measured (110) wave velocities are significantly faster than shock wave velocities from longer time scale gas gun measurements; hence, it appears that on the 100 ps timescale we observe a primarily elastic wave response. Reported PETN gas gun data top-out at U_P = 1.4 km/s. In the region of our highest obtainable piston velocities, beginning at U_P = 2.0 km/s, TDI wave speeds match-well with theoretical shock wave values. Using experimentally determined second-order elastic constants for PETN the bulk quasi-longitudinal relaxed sound velocity was computed for propagation normal to the (110) plane. The TDI data do not linearly extrapolate back to the uncompressed quasi-longitudinal velocity. Atomic scale properties may change in a nonlinear fashion

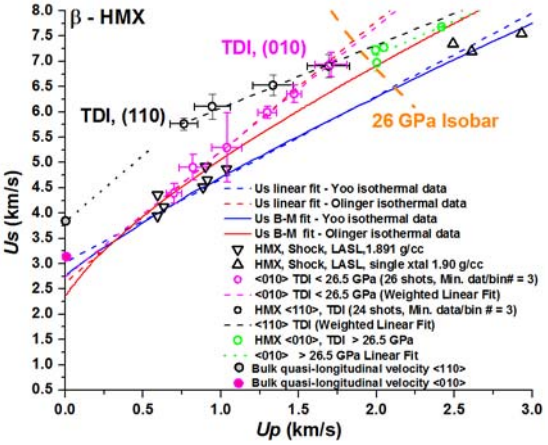

Fig. 7. A comparison of TDI single crystal (110) (010) beta-HMX shock data with previous gas gun data from shocked polycrystalline and single crystal beta-HMX.

when subjected to a high strain fields; hence, here it may not be reasonable to expect a linear trend in pressure or U_P dependent elastic wave speeds.

We conducted ultrafast shock TDI measurements from two different crystallographic orientations of shocked beta-HMX. In Figure 7 we overlay our binned TDI results from (110) and (010) with previous gas gun results. Much like the PETN results, wave velocities normal to the (110) plane may be attributed to elastic compression. Velocities normal to the (010) plane may be from elastic and/or plastic waves where there is good agreement with previous gas gun shock wave measurements up to approximately 12 GPa. For pressures in excess of 12 GPa, ultrafast (010) wave velocities increase linearly along a line that fortuitously agrees with a linear fit of previous hydrostatic pressure-volume measurements. At approximately 26 GPa the rate of increase in (010) TDI wave speeds decrease; and further, they appear to intersect with previous gas gun single crystal (unknown orientation) results. There are only ten published shock wave measurements from beta-HMX. To make additional comparisons we scaled published PBX-9501 shock data (95% beta-HMX, 2.5% estane, 2.5% nitroplasticizer) to a density corrected aggregate bulk quasi-longitudinal sound speed. The bulk modulus of beta-HMX (*Ko* = 13.42 GPa) was computed using experimentally determined second-order elastic

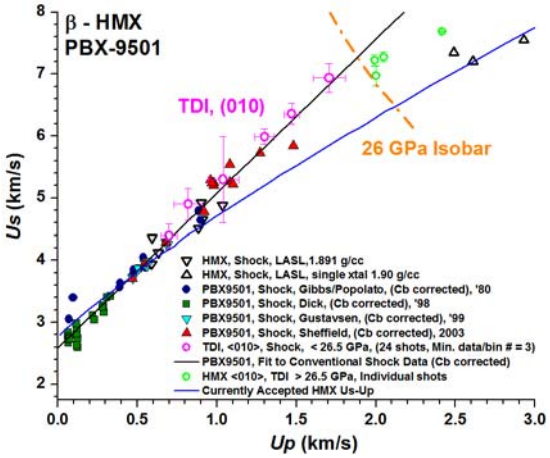

Fig. 8. A comparison of TDI single crystal (010) beta-HMX shock data with density-scaled gas gun data from shocked PBX-9501. The bulk quasi-longitudinal sound-speed of beta-HMX is 2.66 km/s.

constants and then taking the average of the Voight and Reuss elastic compliance models. Knowledge of *Ko* and the difference in density between PBX-9501 and beta-HMX yields a 4% difference in bulk sound velocity. Therefore, we compared TDI wave velocities to +4% scaled PBX-9501 shock velocities (See Fig 8.). Again we observe a perhaps fortuitous agreement between

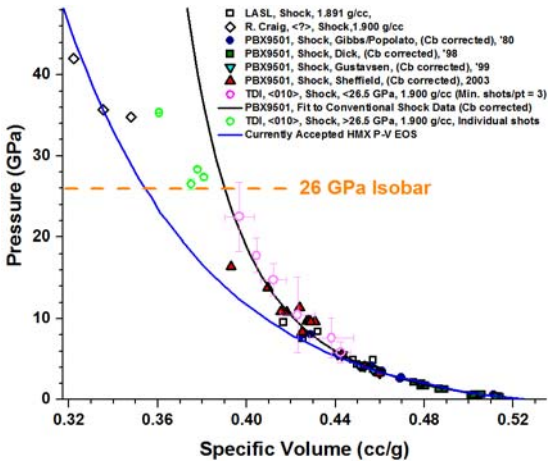

Fig. 9. A comparison of TDI single crystal (010) beta-HMX shock data with density-scaled gas gun data from shocked PBX-9501. The 26 GPa isobar line demarks a known room temperature phase transition.

TDI and scaled gas gun results up to approximately 16 GPa. It is interesting that the TDI and PBX-9501 shock velocities increase linearly while the currently accepted beta-HMX equation of state, (EOS) increases sublinearly The EOS was derived using a 3rd-order Birch-Murnaghan model fit to all 10 shock Hugoniot points and nonhydrostatic cold-compression P-V data. The scaled PBX-9501 data are plotted on the P-V surface in Fig. 9 along with (010) TDI data.

Discussion

PETN

TDI wave velocities from ultrafast shocked single crystal (110) PETN are markedly faster than our previous TDI results for ultrafast shocked polycrystalline PETN. Our polycrystalline PETN results nominally agree with published gas gun data. Therefore we believe there must be a strong elastic component to our single crystal results. We also note that unlike gas gun results, TDI (110) wave velocities do not linearly extrapolate back to the ambient condition bulk quasi-longitudinal velocity. This is not necessarily an unexpected observation because ultrafast shock strain rates are orders of magnitude higher than gas gun strain rates.

Energetic materials are relatively compressible (K_O < 15 GPa) and ultra-high strain fields may result in nonlinear pressure dependent elastic velocities. Indeed, molecular dynamic (MD) shock compression studies (infinite strain rate) of alpha-HMX exhibit nonlinear U_P dependent elastic wave speeds: an elastic wave inflection point in the U_S-U_P plane links two linear trends and it occurs when a plastic wave component nucleates within the crystal. The initial linearly increasing elastic wave velocities exhibit a significantly higher slope than the second linear trend. If we extend these MD observations (10 ps timescale) to the results observed here, it suggests our (110) PETN and beta-HMX elastic wave speeds are all faster than a critical U_P value where wave speeds begin to decrease linearly, with a much steeper slope, to the bulk sound speed. MD results reveal that elastic and plastic wave velocities increase until the plastic wave overtakes the elastic wave resulting in a single over driven plastic wave.

It is possible that our (110) TDI data have a mixture of elastic and plastic wave components where for example at relatively low piston velocities the elastic wave amplitude is significantly higher than the plastic wave and at the highest piston velocities plastic wave is dominate. PETN (110) TDI wave velocities intersect with the unreacted shock Hugoniot (linearly extrapolated) at U_P = 1.7 km/s and also with recent DFT results up to 2.15 km/s (See Fig. 6). With the absence of gas gun data above U_P = 1.47 km/s, one cannot definitively attribute the type of wave(s) we measure in (110) PETN. At piston velocities >1.47 km/s, polycrystalline PETN TDI data including DFT results indicate that the shock Hugoniot is below the linearly extrapolated gas gun line.

The lowest recorded compression (110) PETN time traces reveal what appear to be a plateaus in the intensity phase offset (U_P(t)) that may be blindly interpreted as an elastic to plastic transition in PETN thus signaling the Hugoniot elastic limit

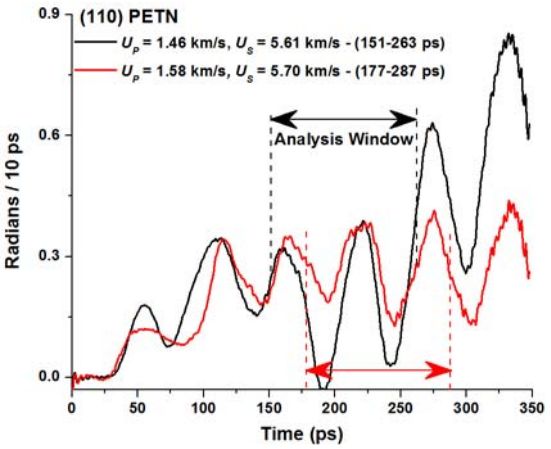

Fig. 10. Time domain interferometry traces from PETN shocked in a direction normal to the (110) plane. The vertical dashed lines (black and red) indicate the region where the data (corresponding solid black and solid red curves) were processed to determine shock and particle velocities. For both shots (black line = # 10053 and red line = #10054) the pump pulse energy was nominally 377 μJ; resulting in markedly different offset intensities or piston velocities.

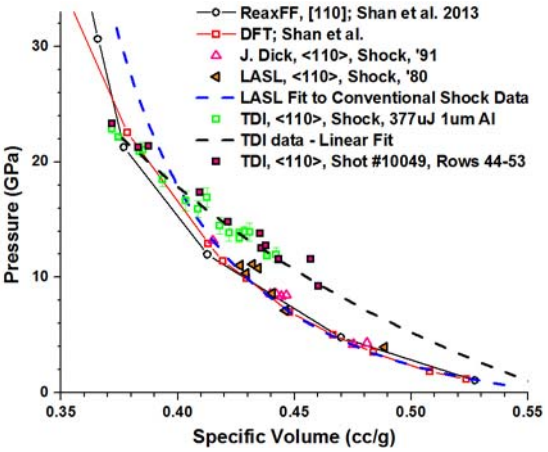

Fig. 11. A comparison of TDI single crystal (110) PETN shock data with previous gas gun data from shocked polycrystalline and single crystal (110) PETN including more recent theoretical results.

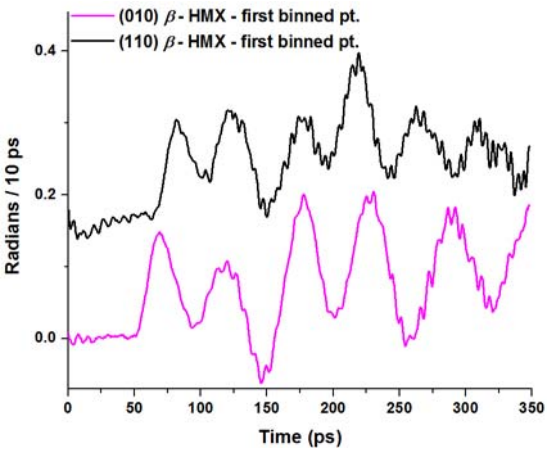

Fig. 12. Time domain interferometry traces from single crystal beta-HMX. To enhance clarity, the (110) trace is shifted upward by 0.15 radians/10ps. Each trace is an average of three single-shot traces. The processed results from each trace are plotted in Figure 7.: they are the lowest piston velocity points (same color coordination). The (110) shock values are, U_P = 0.76 ± 0.09 km/s; U_S = 5.76 ± 0.12 km/s. The (010) shock values are, U_P = 0.70 ± 0.05 km/s; U_S = 4.39 ± 0.19 km/s.

(HEL), which is a parameter that quantifies the strength of a material (See black line in Fig. 10). We rationalize that relatively steady (unstructured) shock waves break out of the ablator. Similar pump pulse energies used to shock tamped aluminum resulted in steady plastic waves breaking out from the free surface of the ablator. At higher PETN compression drives (optical fluence) the time traces have a steady offset at time > 150 ps (See red line in Fig. 10). If indeed higher TDI compression drive data are representative of a plastic or perhaps overdriven plastic wave then for shock stresses > 16 GPa we are measuring unreacted shock Hugoniot states that are at most, ~25 percent higher in shock pressure than previous gas gun results (See Fig. 11).

Beta-HMX

In contrast to (110) velocities, ultrafast (010) beta-HMX results match well with gas gun data below 12 GPa. The corresponding (110) and (010) piston velocities appear to be invariant with the loading direction (See Fig. 12). Low strain rate uniaxial loading experiments normal to the (110) plane reveal that it is the most ductile deformation direction: crystal twins form and an elastic to plastic transition occurs. The mechanical response to loading normal to the (010) plane exhibits no twin formation or twin-slip failure mechanisms.

Therefore, compression normal to (010) will exhibit less ductility: an elastic to plastic response will occur normal to (010) with less strain compared to compression normal to (110). It has also been shown that twin/slip failure dynamics observed at low strain rates also affect deformation phenomena at gas gun strain rates. The (010) HEL would logically occur at a lower piston velocity than the (110) HEL.

The time traces plotted in Figure 12 appear to be steady for U_P > 150 ps: there is no discontinuous jump in piston velocity like that observed in PETN (See Fig. 10.). If the interferograms in Figure 12 are representative of elastic waves, then we would expect to first see an HEL in (010) beta-HMX; indeed, if our interpretations are correct then this is precisely what we observe (See Fig. 13). Going back to the TDI data plotted in Figure 7 and 8, we must reiterate that all of the reported TDI were derived from processing the steadiest components of the time trace wave profiles. No attempt was made to process time dependent displacement in regions where there was a significant increase in

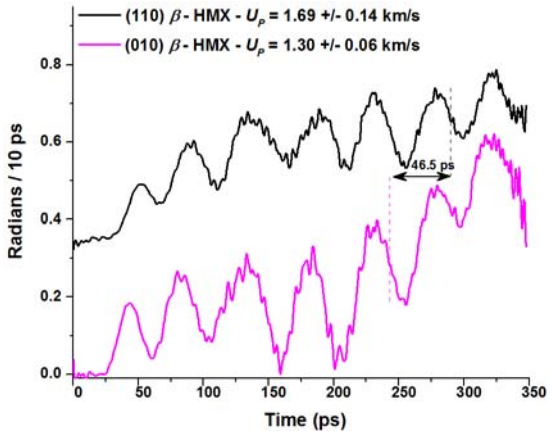

Fig. 13. Single crystal beta-HMX time traces that exhibit the first signatures of what may be loosely interpreted as an elastic to plastic wave transition. To enhance clarity, the (010) line was shifted by +0.35 radians/10 ps. The E-P transition occurs first (lowest piston velocity) with compression normal to the (010) plane. The (010) trace consists of an average of three shots and the (110) trace consists of an average of six shots. The (010) shock velocity is 5.99 ± 0.12 km/s and the (110) shock velocity is 6.91 ± 0.23 km/s.

displacement offset. Clearly such regions would have statistically significant increases in piston velocity. It becomes abundantly clear that a 2x or longer drive duration, with a bit more available drive compression would greatly improve our ability to characterize wave profiles with predominately more plastic deformation.

Summary

The experiments presented in this paper represent our first attempts to elucidate the dynamic response of ultrafast shocked single crystal EMs. It would appear that ultrafast rise time and 350 ps pulse duration shocks are sufficient to characterize the elastic response of ultrafast shocked single crystal EMs; however, in order to more confidently extend measurements of unreacted shock Hugoniot states (propagating in an arbitrary direction) we will need to lengthen our pulse duration to perhaps 700 ps.

The divergence observed between TDI elastic wave results and the accepted beta-HMX EOS will be reduced when we in fact measure plastic wave velocities; but, will there be near complete agreement? A comparison between ultrafast TDI (010) beta-HMX measurements (most probably elastic waves) with the density scaled PBX-9501 EOS reveals a fortuitously good agreement up to a shock stress of 16 GPa. At 16 GPa the PBX-9501 EOS is significantly stiffer than the currently accepted beta-HMX EOS. Our TDI data and the PBX-9501 EOS may indicate that the currently accepted beta-HMX EOS will need to be corrected: it is based partly on just 10 shock Hugoniot points where the three highest pressure point values are most likely affected by a phase transition. Our ultrafast shock compression work on solid-phase EMs will continue. We will lengthen the drive duration of our experiment by >2x and will also have available more laser energy required to achieve higher shock stress states.

Acknowledgements

We acknowledge financial support from the DOE/LLNL High Explosives Science Campaign-II. This work was performed under the auspices of the U.S. Department of Energy jointly by Lawrence Livermore National Laboratory under Contract DE-AC52-07NA27344.

References

1. Armstrong, M. R., Crowhurst, J. C., Bastea, S., & Zaug, J. M., "Ultrafast observation of shocked states in a precompressed material," *J. Appl. Phys.* Vol. 108, pp. 023511, 2010.

2. Armstrong, M. R., Crowhurst, J. C., Bastea, S., & Zaug, J. M., "Observation of off-Hugoniot shocked states with ultrafast time resolution" *Proceedings of the14th International Detonation Symposium*, pp. 435-443, Coeur d'Alene, ID. 2010.

3. Marsh, Stanley P. LASL Shock Hugoniot Data. pp. 482,618, U. of California Press: Berkeley, CA, 1980.

4. Dick, J. J., Mulford, R. N., Spencer, W. J., Pettit, D. R., Garcia, E. and Shaw, D. C., "Shock Response of Pentaerythritol Tetranitrate Single Crystals," *J. Appl. Phys.* Vol. 70, pp 3572, 1991.

5. Shan, T.-R., Wixom, R. R., Mattsson A. E. and Thompson A. P., "Atomistic Simulation of Orientation Dependence in Shock-Induced Initiation of Pentaerythritol Tetranitrate," *J. Phys. Chem. B* Vol. 117, pp. 928-933, 2013.